

Original Article

Exercise improves systemic metabolism in a monocrotaline model of pulmonary hypertension

Ganesha Poojary^a, Sampara Vasishta^b, R. Huban Thomas^c, Kapaettu Satyamoorthy^d,
Ramachandran Padmakumar^e, Manjunath B. Joshi^b, Abraham Samuel Babu^{a,*}

^a Department of Physiotherapy, Manipal College of Health Professions, Manipal Academy of Higher Education, Manipal, Karnataka, 576104, India

^b Department of Ageing Research, Manipal School of Life Sciences, Manipal Academy of Higher Education, Manipal, Karnataka, 576104, India

^c Department of Anatomy, Kasturba Medical College Manipal, Manipal Academy of Higher Education, Manipal, Karnataka, 576104, India

^d SDM College of Medical Sciences and Hospital, Shri Dharmasthala Manjunatheshwara (SDM) University, Manjushree Nagar, Sattur, Dharwad, Karnataka, 580009, India

^e Department of Cardiology, Kasturba Medical College, Manipal Academy of Higher Education, Manipal, Karnataka, 576104, India

ARTICLE INFO

Keywords:

Pulmonary arterial hypertension

Monocrotaline model

Metabolites

Metabolomics

Endothelial dysfunction

Exercise

ABSTRACT

Exercise training in pulmonary arterial hypertension (PAH) has been gaining popularity with guidelines now recommending it as an important adjunct to medical therapy. Despite improvements in function and quality of life, an understanding of metabolic changes and their mechanisms remain unexplored. The objective of this study was therefore to understand the metabolic basis of exercise in a monocrotaline model of PAH.

24 male Wistar rats (age: 8–12 weeks and mean body weight: [262.16 ± 24.49] gms) were assigned to one of the four groups (i.e., Control, PAH, Exercise and PAH + Exercise). The exercise groups participated in treadmill running at 13.3 m/min, five days a week for five weeks. Demographic and clinical characteristics were monitored regularly. Following the intervention, LC-MS based metabolomics were performed on blood samples from all groups at the end of five weeks. Metabolite profiling, peak identification, alignment and isotope annotation were also performed. Statistical inference was carried out using dimensionality reducing techniques and analysis of variance.

Partial-least-squares discrimination analysis and variable importance in the projection scores showed that the model was reliable, and not over lifting. The analysis demonstrated significant perturbations to lipid and amino acid metabolism, arginine and homocysteine pathways, sphingolipid ($p < 0.05$), glycerophospholipid ($p < 0.05$) and nucleotide metabolism in PAH. Exercise, however, was seen to restore arginine ($p < 0.05$) and homocysteine ($p < 0.0001$) levels which were independent effects, irrespective of PAH.

Dysregulated arginine and homocysteine pathways are seen in PAH. Exercise restores these dysregulated pathways and could potentially impact severity and outcome in PAH.

1. Introduction

Pulmonary arterial hypertension (PAH) manifests due to abnormal pulmonary vascular changes characterized by endothelial dysfunction, aberrant proliferation of fibroblasts and smooth muscle cells. These cellular changes lead to excessive and progressive vasoconstriction leading to adverse vascular remodelling.¹ Pre-clinical and clinical studies have demonstrated that age, female gender, toxin exposure, genetic variants, and existing comorbid conditions predispose to PAH.² Often, PAH has been noted as a final (patho)physiological process as a consequence of disparate set of diseases such as atrial fibrillation,

cardiomyopathy and deep vein thrombosis.³ PAH impairs the normal exchange of oxygen and carbon dioxide in the lungs, leading to a reduced oxygen supply to the tissues. Subsequently, reduced oxygenation affects the mitochondria's ability to efficiently generate ATP, compromising the energy production necessary for muscle function during exercise, which concomitantly influences downstream metabolism. Such mitochondrial dysfunction leads to significant metabolic reprogramming in both tissue/organ and systemic levels.⁴ Hypoxia, inflammation, and metabolic stress activate Hypoxia-Inducible Factor (HIF)-1 α and HIF-2 α transcription factors^{5,6} that leads to increased glycolysis and reduced glucose oxidation, reflecting a Warburg effect of cancer cells in pulmonary vascular cells.⁷ Both animal and clinical models of PAH have

* Corresponding author.

E-mail addresses: abrahambabu@gmail.com, abraham.babu@manipal.edu (A.S. Babu).

<https://doi.org/10.1016/j.smhs.2024.03.001>

Received 12 October 2023; Received in revised form 4 February 2024; Accepted 4 March 2024

Available online 8 March 2024

2666-3376/© 2024 Chengdu Sport University. Publishing services by Elsevier B.V. on behalf of KeAi Communications Co. Ltd. This is an open access article under the CC BY-NC-ND license (<http://creativecommons.org/licenses/by-nc-nd/4.0/>).

Abbreviations

PAH	Pulmonary arterial hypertension
LC-MS	Liquid chromatography-mass spectrometry
MCT	Monocrotaline
PDGF	Platelet-derived growth factor
PASMC	Pulmonary arterial smooth muscle cells
HMDB	Human metabolome database
HIF	Hypoxia-inducible factor
HRMS	High-resolution mass spectrometry
CHD	Congenital heart disease
PLS-DA	Partial-least-squares discrimination analysis

LysoPA	Lysophosphatidic acid
LysoPC	Lysophosphatidylcholines
LysoPE	Lysophosphatidylethanolamine
PG	Phosphatidylglycerol
DAG	Diacylglycerol
MAG	Monoacylglycerol
AMPK	AMP-activated protein kinase
NO	Nitric oxide
eNOS	Endothelial nitric oxide synthase
ADMA	Asymmetric dimethylarginine
gms	Grams

demonstrated the Warburg phenotype.^{8–16} Where HIF-1 α activates expression of pyruvate dehydrogenase kinases 1 and 2 (PDK1/2) which reduce pyruvate dehydrogenase-mediated (PDH-mediated) pyruvate to acetyl-CoA conversion.^{8,17} Recent plasma metabolomics analysis in 117 PAH participants revealed distinct metabolite profiles which correlated with right ventricle dilation, mortality, and severity of disease.¹⁸ The authors observed modulations in polyamine, histidine, and sphingomyelin metabolism intermediates, which served as better markers for identifying patients at risk for poor prognosis.¹⁸ In another study, HRMS (High-resolution mass spectrometry) analysis of plasma indicated perturbations in lipid metabolism and fatty acid oxidation pathways.¹⁹ Using a targeted metabolomics approach, He et al. (2020) demonstrated elevated spermine levels in idiopathic PAH subjects and inhibition of spermine synthase, which in turn reduced Platelet-derived growth factor (PDGF) induced proliferation of Pulmonary arterial smooth muscle cells (PASMCs) and ameliorated monocrotaline mediated PAH in rats.²⁰

Individuals with PAH often experience exercise intolerance, fatigue, and shortness of breath during physical exertion.²¹ Initial studies pointed out that exercise training in PAH subjects worsens clinically and however, mounting evidence including our own studies, indicates exercise improves functional capacity and hence clinically explored as rehabilitation in PAH.^{22,23} The present study aimed to understand the metabolic basis of exercise in PAH models. Further, the identification of relevant metabolic targets that correspond with exercise capacity, a well-established marker of disease severity, is made possible by examining metabolism during exercise. Evaluation of pulmonary vascular metabolism during exercise is anticipated to offer significant benefits since dysregulated metabolism reflects pulmonary vascular remodelling, which in turn affects pulmonary vascular and RV reserves. Hence, in the present study exploring LC-MS-based untargeted metabolomics approach, we examined a) metabolic alterations in PAH animal models and b) interrogated whether exercise restores altered metabolism in PAH.

2. Methods**2.1. Animal ethics, animal house conditions, identification of animal, grouping**

The study was initiated after obtaining approval from the Animal Ethics Committee of Kasturba Medical College, Manipal Academy of Higher Education, Manipal (IAEC/KMC/41/2019). Male Wistar rats (*Rattus norvegicus*) aged between 8 and 12 weeks, with body weight ranging between 216 and 296 gms, were obtained from the Central Animal Research Facility. Single animals per cage/sex were housed in the standard polysulfone cages (Size: approximately L 425 mm \times B 266 mm \times H 185 mm), with stainless steel top grill having facilities at the central animal facility and were fed with standard food, water ad libitum and air-conditioned with adequate fresh air supply. The laboratory environment was maintained with a temperature of 21 $^{\circ}$ C–23 $^{\circ}$ C and 12 hours (h) light and 12 h dark cycle was maintained. For bedding material steam

sterilized rice husk was used and changed along with the cage at least once a week (\pm 1 day). The identification of individual rats was done by cage card containing rat accession number. The temporary body marking during the acclimatization period was done with crystal violet. During grouping turmeric colour body markings were made and animals were systematically randomized based on body weight stratification. Research scholars are aware of the group allocation at the different stages of the experiment. "The study is reported in accordance with the Animal Research: Reporting In Vivo Experiments (ARRIVE) guidelines 2.0".²⁴ (Supplemental Table 1 and 2).

2.2. Induction of PAH and exercise protocols

Twenty-four animals ($n = 6$ in each group) were prospectively randomized into four groups. They were control (which did not receive any intervention for the entire duration of the experiment), PAH (which were induced with PAH and then did not receive any intervention for the duration of the experiment), Exercise (healthy animals subject to moderate intensity exercise), and PAH + Exercise (PAH animals subject to moderate intensity exercise). (Supplemental Table 3).

PAH was induced using the monocrotaline (MCT) model. Animals were administered a single dose of 60 mg/kg body weight of MCT (MedChemExpress LLC, USA) subcutaneously on day 1 of the experimental period. Based on the onset of clinical signs (lethargy, weight loss, and reduced activity), we identified the onset of PAH. Once animals developed signs of the onset of PAH, they were processed for exercise intervention. Considering exercise training as a new task, animals were familiarized for one week prior to induction of PAH. This helped the animals acclimatize to the treadmill environment. Animals were made to run on an 800 series rodent treadmill (IITC, Inc. Life Science, USA) at 13.3 m/min with no inclination²⁵ for 20–30 minutes (min) per day, 5 days a week. Once PAH was induced, animals continued the same exercise training protocol for five weeks. Exhaustion was established when the animal could no longer run on the treadmill or received three consecutive electric stimuli. A summary of the entire process is summarized in Fig. 1. At the end of the experiment, all rats were euthanized using ketamine/xylazine anaesthesia. Organs were then harvested after perfusion with saline and fixative and subjected to detailed necropsy. Particular attention was given to any changes in the lungs and heart tissues. Plasma was separated from blood and frozen at -80° C after snap freezing in liquid nitrogen.

2.3. Morphometric analyses

Histopathological examination of the right lung near the hilum of all the experimental groups. The right lungs obtained from all experimental groups ($n = 6$) were paraffin-embedded, sectioned at 4 μ m, and stained with hematoxylin and eosin. The pulmonary artery of each group of animals were identified and analysed for histopathological changes.

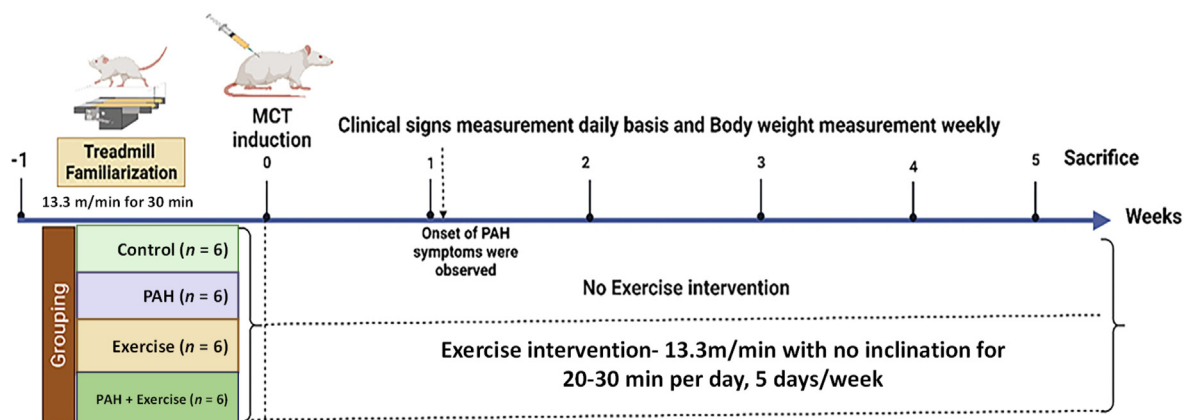


Fig. 1. Shows schematic of study conducted. This study was designed to identify the metabolites released through exercise in a control model and a PAH model. This will utilize Wistar Rats divided into four groups (i.e., a) Control ($n = 6$), b) PAH ($n = 6$) c) Exercise ($n = 6$), and d) PAH + Exercise ($n = 6$). Animals were systematically randomized based on body weight stratification before PAH induction. PAH was induced using monocrotaline. Clinical signs were recorded daily, and body weight was measured weekly basis. Blood samples were drawn at baseline and after 5 weeks. At the end of the experiment, all rats were sacrificed.

2.4. Untargeted LC-MS analysis

2.4.1. Metabolite extraction

The metabolite extraction was performed as reported in our previous manuscript.²⁶ The 200 μL of ice-cold, mass-spec grade methanol was added to the 100 μL of plasma sample, vortexed for 10 seconds (s), and centrifuged for 10 min at 13 200 rpm. The supernatant was vacuum dried, and the pellet was dissolved in 90% acetonitrile and 0.1% formic acid and processed for mass spectrometry analysis.

2.4.2. Metabolomics analysis

The liquid chromatography-electrospray ionization-quadrupole-time of flight-mass spectrometry (Agilent 6520, Santa Clara, USA) connected to a liquid chromatography system (Agilent 1200 Santa Clara, USA) was used for metabolite profiling. The samples were run in positive mode at a 0.4 mL/min flow rate, 50–1 700 m/z scan range, and 1.4 spectra/s scan rate. The sample was dissolved in 20 μL of water: acetonitrile (95:5) solvent solution that included 0.1% formic acid, and 8 μL of that solution was passed using an autosampler onto a Phenomenex column (Kinetex C18, 5 μm). Mobile phase A consisted of 90% mass spectroscopy grade water and Mobile phase B was acetonitrile (90%) and 0.1% formic acid. The Mass spectrometry (MS) was set to scan with reference masses of 121.050873 and 922.009798 with a gas temperature of 250 $^{\circ}\text{C}$ and with the ESI capillary voltage set at 3 500 V. The pressure of the nebulizer was fixed at 40 psig and the gas flow was maintained at 8 L/min. Additionally, MS/MS was carried out to determine the parent and daughter ions.

2.5. Data processing and Statistical analysis

The raw data files (.d) were converted into mzXML using Proteowizard msConvert software. The files were further analysed using the on-line tool XCMS Online²⁷ for peak identification, alignment, and isotope annotation after being converted to the mzXML format using ProteoWizard.²⁸ In XCMS Online, the following settings were made following a prior study²⁹: feature detection settings were with a m/z tolerance limit of 15 ppm and peak width time frame of (10 s–60 s); all other parameters were left at their preset values. After the data was normalised, an Excel feature table with each feature's m/z , retention time, and abundance for each sample had been created. The multivariate analysis included dimensionality reducing techniques such as principal component analysis (PCA) and t -tests (assume unequal variance, $\alpha = 0.05$) were conducted on the peak areas. Following processing, a peak list was produced that included the peak intensity, retention period, and mass-to-charge ratio (m/z). Using the HMDB online database features with $p < 0.05$

were classified as differentially altered metabolites and subsequently identified based on the precise molecular weight and the similarity of the MS/MS spectra. By comparing the precision of the m/z value (15 ppm) in the MS/MS spectra, the compounds of the metabolites were identified. The remaining features were loaded into MetaboAnalyst 5.0 to perform pathway analysis and MS-DIAL software was used to identify the metabolites' peak for MS/MS analysis.

The mean and standard error of all test group data were calculated using the experiment's total number of animals. Analysis of variance (ANOVA) was used to examine the data in both one- and two-way formats. To compare individual means, post-hoc analysis using Tukey's test was run. Statistical significance was determined using a predefined threshold of p -value ≤ 0.05 . Data analysis and result visualization were performed using GraphPad Prism version 8.00 for Windows, developed by GraphPad Software based in La Jolla, California, USA.

3. Results

3.1. Development of PAH rodent model

As a first step, we developed PAH and exercise training models. PAH was confirmed by the onset of clinical signs such as anorexia, listlessness, weakness, diarrhoea, tachypnea, and changes in body weight, which were seen in all 12 PAH animals from PAH and PAH + Exercise group (Supplemental Table 4, Supplemental Fig. 1A&B). Clinical signs including anorexia, failure to gain weight, and tachypnea were observed in the PAH animals 3–7 days following induction of PAH (Supplemental Fig. 1A). At the end of five weeks, the average body weight of the PAH animals was significantly reduced ($p < 0.0001$) from the control. However, exercise in PAH showing a lesser magnitude of weight loss ($[89.92 \pm 21.79]$ g) compared to PAH group (Supplemental Fig. 1B and Supplemental Table 4). PAH-induced changes were further confirmed by histopathology of the pulmonary artery which revealed thickening in the tunica intima, media, and adventitia of the pulmonary arterial wall (Fig. 2B). Histopathological changes of the pulmonary artery in each group are shown in Fig. 2. Differences were observed between the PAH and non-PAH groups (Fig. 2B&D). These findings intrigued us to carryout metabolomics analysis to identify the metabolic basis of exercise-induced beneficial effects in PAH models.

3.2. PAH and exercise induce significant systemic metabolic reprogramming

Our untargeted metabolomics analysis revealed the presence of 2 745

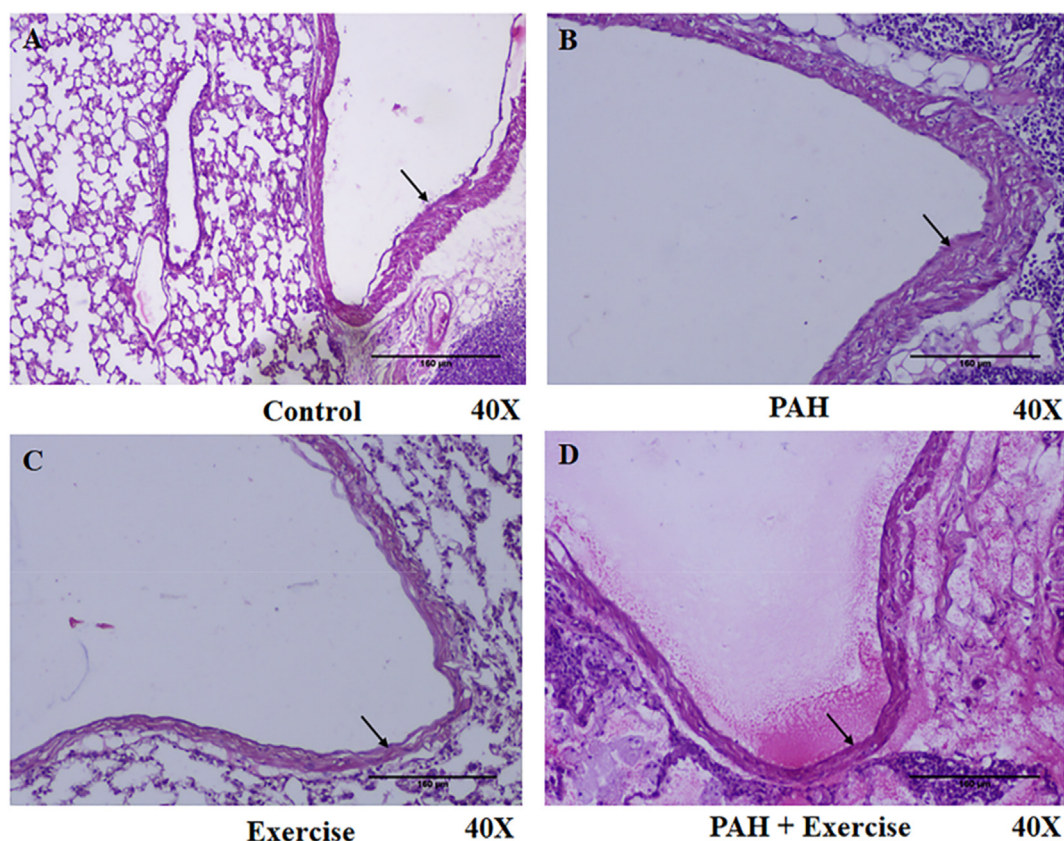


Fig. 2. Histopathological characterization of PAH animals. Representative histopathological images of rat right lung tissues stained by Hematoxylin and eosin are provided (40X). A) Control ($n = 6$), B) PAH ($n = 6$), C) Exercise ($n = 6$) & D) PAH + Exercise ($n = 6$). Pulmonary artery is indicated by the arrow mark. (Scale bars = 160 μm).

spectral features across all groups. Further analysis revealed 190 metabolites that were commonly found across all four groups. HMDB-based annotation and biochemical characterization of these 190 metabolites indicated 110 lipids (57.9%), 36 amino acids & derivatives (18.9%), 22 nucleotides (11.6%), 10 xenobiotics (5.3%), 3 hormones (1.6%), 3 carbohydrates (1.57%), 5 vitamins (2.6%) and 1 polyamine (0.5%) (Fig. 3E).

A total of 180/190 endogenous metabolites were considered for the analysis (10 xenobiotics [5.3%] were excluded from the study) and these metabolites were validated through MS/MS analysis of their m/z values and fragmentation patterns, ensuring the validation of the annotated compounds. Comparison between the Control and PAH groups showed 121 compounds were significantly altered (i.e., 25 upregulated and 96 downregulated) (Fig. 5B). Similarly, a comparison between the Control and Exercise group indicated 126 compounds that were significantly altered of which 92 were significantly upregulated and 34 downregulated (Fig. 5A). When PAH and PAH + Exercise groups were compared, only 2/180 compounds were found to be significantly downregulated and 126 were upregulated (Fig. 5C). (Note: In PAH group, 2 animal data points were not included in the analysis. PAH + Exercise group, one animal data point was not included in the analysis because in the PAH group rat No. 7 died on day 30 and on day 38 animal No. 10 was dead. In the PAH + Exercise, rat No.23 died on day 35).

3.3. PAH and exercise induced animals show distinct plasma metabolic patterns

Partial-least-squares discrimination analysis (PLS-DA) was used (Fig. 3A) for multivariate analysis to identify metabolites that significantly contributed to the classification of the animals and to remove the effect of inter-animal variability. The PLS-DA score plots demonstrated a distinct differentiation between the control group and the PAH, Exercise,

and PAH + Exercise groups when all experimental groups were combined. Component 1 accounted for 13.7% of the total variation, while component 2 explained 27% of the variation (Fig. 3. A). However, to distinguish precise variations, we performed PLSDA analysis for all the groups with respect to control. We observed during PLSDA that component 1 accounted for 36.7% of the total variation, and component 2 explained 28% of the variation when comparing the Control and Exercise group (Fig. 3. B). For the Control Vs PAH group, Component 1 accounted for 29.6% of the total variation, while component 2 explained 33.9% of the variation (Fig. 3C). Finally, for the PAH vs PAH + Exercise group, Component 1 accounted for 32.2% of the total variation, while component 2 explained 27.8% of the variation. (Fig. 3D). This separation suggests that there are significant differences in the measured variables between the control group and the PAH, Exercise, and PAH + Exercise groups. The variable importance in the projection (VIP) scores from the PLS-DA model was used to rank the metabolites, and typically, metabolites with VIP values > 1.0 were considered as major contributors. All four groups showed distinct distributions in the PLS-DA plot, which indicated that the model was reliable, and not over lifting (Fig. 3A).

3.4. Exercise influences metabolism in healthy rats

The metabolite levels of DG (2:0/22:6(5Z,8E,10Z,13Z,15E,19Z)-2OH(7S,17S)/0:0) ($p < 0.05$) were significantly increased in response to exercise. LysoPA (18:0/0:0), LysoPE(0:0/18:3[9Z,12Z,15Z]) ($p < 0.05$), and LysoPC(P-16:0/0:0) were elevated in response to exercise when compared with the control group. Similarly, exercise exerted effects on the levels of steroid conjugate such as Cholesterol sulfate and linoleic acid (Fig. 4 A, B & Fig. 5A). D - Glucose ($p < 0.001$) was reduced in response to exercise when compared with the control. Amino acids such as L-Serine ($p < 0.05$), L-Histidine ($p < 0.05$), L- Arginine ($p < 0.05$), and L-

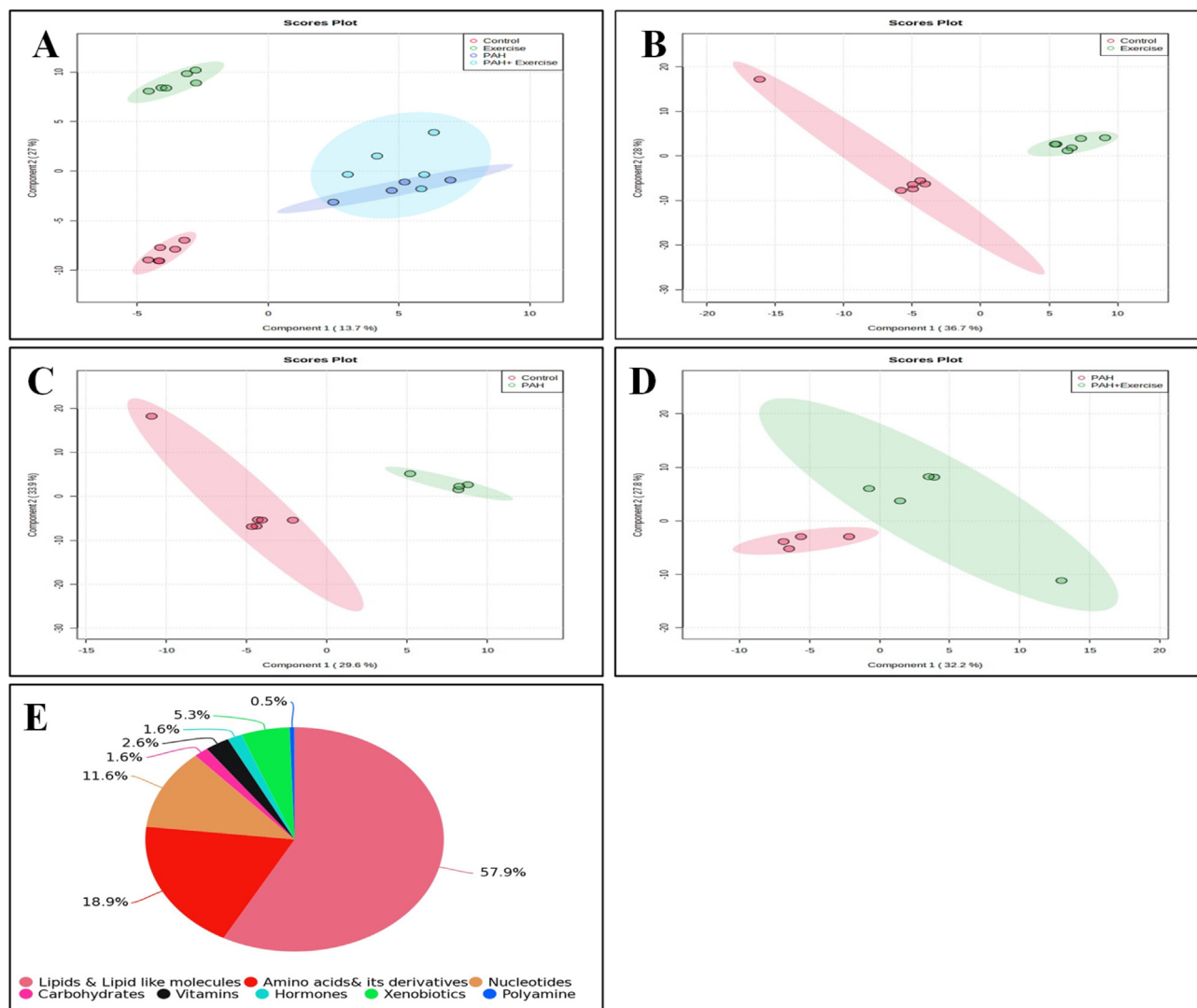


Fig. 3. Metabolic characterization of PAH animals. A) Image shows 2D Score plot Partial Least Squares Discriminant Analysis (PLS-DA) representing distinct metabolite profiles across 4 different groups (Red colour: Control [$n = 6$], Green colour: Exercise [$n = 6$], Blue colour: PAH [$n = 4$], and Sky blue colour: PAH + Exercise [$n = 5$]). B-D) Image shows a 2D Score plot PLS-DA representing distinct metabolite profiles across 2 different groups. B) Control Vs Exercise (Red colour: Control [$n = 6$], Green colour: Exercise [$n = 6$]). C) Control Vs PAH (Red colour: Control [$n = 6$], Green colour: PAH [$n = 4$]). D) PAH vs PAH + Exercise (Red colour: PAH [$n = 4$], Green colour: PAH + Exercise [$n = 5$]). E) A pie chart depicting the classification of metabolites based on their biochemical characterization.

Phosphoarginine ($p < 0.05$) were significantly increased because of the exercise. Our data also showed that Pantetheine 4'-phosphate ($p < 0.001$) levels was significantly reduced in the exercise rats (Figs. 4C and 5A). Cytosine ($p < 0.05$), 5-Methylcytosine ($p < 0.0001$), Uridine 5'-diphosphate ($p < 0.05$), Adenosine monophosphate ($p < 0.001$), 1-Methyladenine ($p < 0.001$) and niacinamide ($p < 0.05$) were significantly increased in response to exercise when compared with the control group. However, we also observed increasing levels of hypoxanthine ($p < 0.05$), uric acid ($p < 0.05$), and guanine ($p < 0.05$) in the exercise group (Figs. 4D and 5A).

3.5. MCT treatment shows significant perturbations in lipid and amino acid metabolism

Metabolome analysis of MCT-induced PAH models showed significant metabolite reprogramming. Lipid and amino acid metabolism pathways were significantly altered upon induction of PAH. Under the category of eicosanoids, we observed a significant decrease in Leukotriene B4 ($p < 0.05$), prostaglandin C2 ($p < 0.05$), and prostaglandin E2 ($p < 0.05$). However, thromboxane A2 ($p < 0.0001$) and prostaglandin G2 levels were

increased when compared to controls. Sphingolipids including Cer(d18:0/16:0) ($p < 0.05$), sphingosine ($p < 0.05$), sphinganine ($p < 0.05$), sphinganine 1-phosphate ($p < 0.0001$) and sphingosine 1-phosphate ($p < 0.05$) were decreased in the PAH group (Fig. 4A, B & Fig. 5B). Further, we observed a derailment in the glycerolipids in response to the MCT treatment. The levels of the MG (0:0/i-16:0/0:0) ($p < 0.05$) and DG(2:0/22:6(5Z,8E,10Z,13Z,15E,19Z)-2OH(7S,17S)/0:0) ($p < 0.05$) were reduced. Monoglycerides levels were unaltered whereas the levels of DG(PGF1alpha/2:0/0:0) ($p < 0.001$) were significantly increased in PAH (Fig. 4A, B & Fig. 5B). Several subclasses of glycerophospholipids such as Phosphatidylglycerol (PG), Lysophosphatidic acid (LysoPA), Lysophosphatidylcholines (LysoPC), and lysophosphatidylethanolamine (LysoPE) were altered in response to MCT treatment. LysoPA (18:0/0:0) ($p < 0.05$), LysoPC(P-16:0/0:0) ($p < 0.05$), LysoPE(0:0/18:3[9Z,12Z,15Z]) ($p < 0.05$) were reduced in MCT treated rats. The Phosphatidylglycerol (PG) such as PG (22:6[4Z,8Z,10Z,13Z,16Z,19Z]-OH(7)/i-12:0) ($p < 0.0001$) was significantly reduced whereas PG(PGJ2/i-14:0) ($p < 0.001$) levels were significantly increased. The metabolites including Palmitic acid ($p < 0.001$), which is a 16-carbon chain saturated fatty acid, linoleic acid ($p < 0.0001$), and arachidonic acid ($p < 0.0001$) which are omega - 6

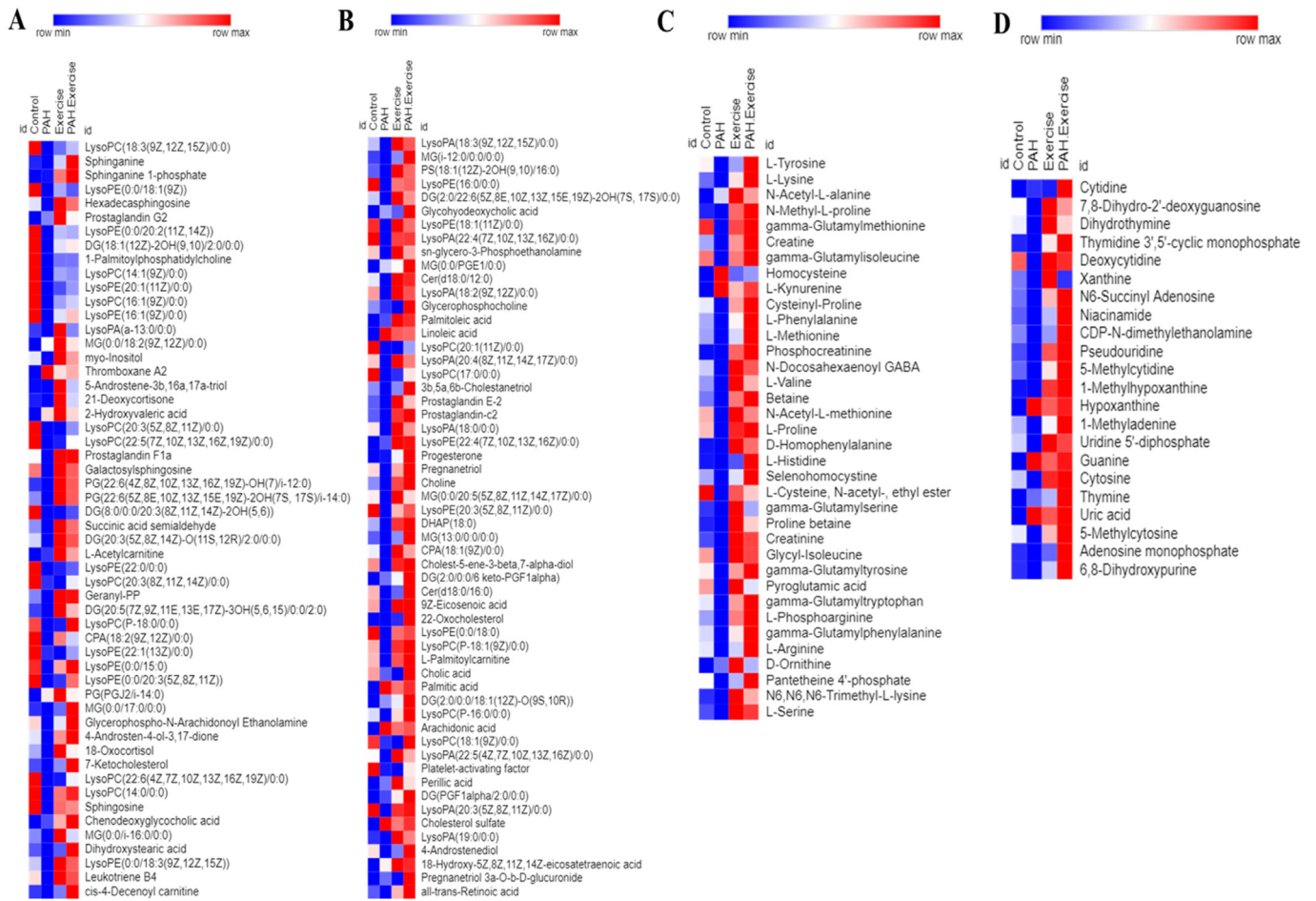


Fig. 4. PAH and exercise reprograms metabolism. Heat map representing differential abundance of Lipids (A & B), Amino acids (C) and Nucleotides (D) across 4 different groups (Control [$n = 6$], PAH [$n = 4$], Exercise [$n = 6$] & PAH + Exercise [$n = 5$]). The red colour indicates rise in mean metabolite abundance, while blue colour indicates reduction in mean metabolite abundance.

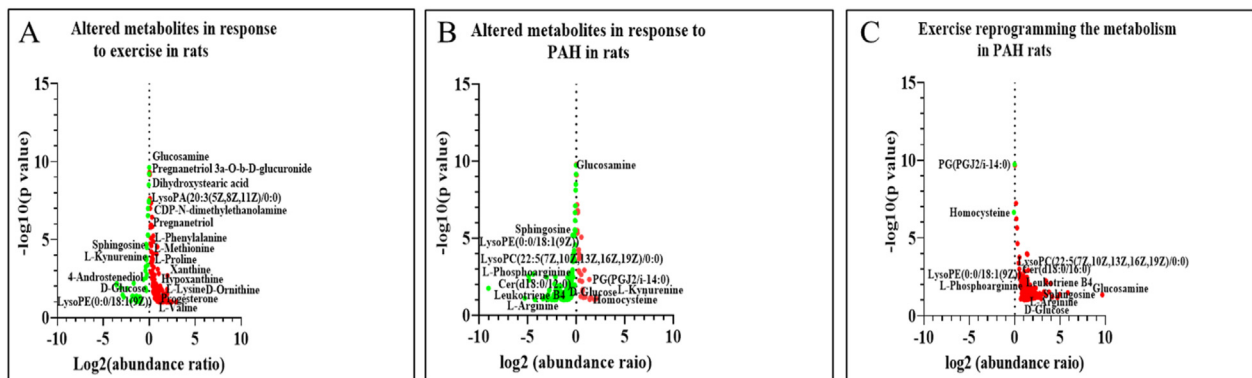


Fig. 5. Volcano plots representing the altered metabolites in response to A) Exercise ($n = 6$), B) PAH ($n = 4$) and C) PAH + Exercise ($n = 5$) based on $\log_2(\text{abundance ratio})$ and $-\log_{10} P$ value. The red circle indicates upregulation of metabolites and green circle indicates downregulation of metabolites.

polyunsaturated fatty acids with 18 and 20 carbon chains respectively were increased in the MCT treated group when compared with the control. PAH animals showed a significant increase in cholesterol sulfate ($p < 0.0001$), which is a steroid conjugate (Fig. 4 A, B & Fig. 5 B). With respect to carbohydrate metabolism, D-glucose was reduced and its amino sugar derivative, glucosamine was increased in the PAH group (Fig. 5 B).

L-Serine, L-Lysine ($p < 0.05$), L-Arginine ($p < 0.05$), L-Valine ($p < 0.05$), and L-phenylalanine ($p < 0.05$), levels were significantly decreased in the PAH rats. Homocysteine ($p < 0.05$), methionine

metabolism intermediate, tryptophan metabolite L-Kynurenine, and D-Ornithine ($p < 0.05$), an intermediate of the urea cycle were significantly elevated in the PAH group (Figs. 4C and 5 B). The intermediates of pyrimidine metabolism such as Cytosine ($p < 0.05$) and its modified form 5-Methylcytidine ($p < 0.05$), 5-Methylcytosine ($p < 0.05$), Uridine 5'-diphosphate ($p < 0.05$), and Thymidine 3',5'-cyclic monophosphate ($p < 0.05$) was significantly decreased in PAH group in comparison to the control group. The purines including Adenosine monophosphate ($p < 0.0001$) and its methylated form 1-Methyladenine ($p < 0.05$),

Xanthine ($p < 0.05$), and 1-Methylhypoxanthine ($p < 0.0001$) were significantly reduced in PAH. However, Guanine ($p < 0.0001$), hypoxanthine ($p < 0.05$), and uric acid ($p < 0.05$), which is an end product of the purine catabolism were increased in the PAH group (Figs. 4D and 5B).

3.6. Exercise improves deranged metabolism in PAH animals

The levels for the majority of intermediates in lipid metabolism were restored as a result of exercise in PAH animals. Leukotriene B4 ($p < 0.05$), an eicosanoid and sphingolipids including Cer(d18:0/16:0) ($p < 0.05$), sphingosine ($p < 0.05$), sphinganine ($p < 0.05$), sphinganine 1-phosphate ($p < 0.05$) and sphingosine 1-phosphate ($p < 0.05$) which were decreased in the PAH group was restored upon Exercise. The DG (2:0/22:6(5Z,8E,10Z,13Z,15E,19Z)-2OH(7S,17S)/0:0) ($p < 0.05$), diacylglycerol which is a category of glycerolipids was significantly increased in the PAH + Exercise group. We observed a significant decrease in PG(PGJ2/i-14:0) ($p < 0.001$) which was increased in PAH. Exercise on the other hand, increased the levels of LysoPA (18:0/0:0) ($p < 0.05$), lysoPC(P-16:0/0:0) ($p < 0.05$), and LysoPE(0:0/18:3(9Z,12Z,15Z)) ($p < 0.05$) when compared to the PAH group. The increased levels of Palmitic acid, Arachidonic acid, Linoleic acid, and Cholesterol sulfate remained unchanged despite exercise (Fig. 4A, B & Fig. 5C). Furthermore, exercise had no effect on the metabolic intermediates of carbohydrates such as glucosamine and D-glucose in PAH (Fig. 5C). The exercise was seen to increase amino acids and their metabolic intermediates associated with vascular functions. L-Serine ($p < 0.05$), L-Arginine ($p < 0.05$), and L-Phosphoarginine ($p < 0.05$) were significantly elevated because of exercise. Exercise significantly reduced levels of Homocysteine ($p < 0.0001$) in PAH animals. However, no changes were observed in the levels of ornithine and tryptophan metabolite kynurenine in response to exercise (Figs. 4C and 5C). The exercise produced an increase in the levels of

pyrimidines and their modified forms such as Cytosine ($p < 0.05$), 5-Methylcytosine ($p < 0.05$), and Uridine 5'-diphosphate ($p < 0.05$). The purine metabolism intermediates such as Adenosine monophosphate ($p < 0.05$), 1-Methyladenine ($p < 0.05$), and 1-Methylhypoxanthine ($p < 0.05$) also increased with exercise (Figs. 4D and 5C).

The MetaboAnalyst 5.0 was used to perform pathway analysis on the annotated metabolites. The KEGG pathway database identified 11 significant pathways (Supplemental Table 5 and Fig. 6). These metabolites corresponded to, Glycerophospholipid metabolism, Pyrimidine metabolism, Sphingolipid metabolism, Arachidonic acid, Arginine and proline metabolism, Purine metabolism pathway, and Steroid hormone biosynthesis pathway (Figs. 6 and 7).

4. Discussion

In the present study we aimed to understand the metabolic basis of a) PAH pathogenesis and b) whether altered metabolism was restored upon exercise training in rat models of monocrotaline-induced PAH. Our LC-MS-based untargeted metabolomics analysis revealed that PAH altered metabolic intermediates of glycerophospholipid, purine and pyrimidine, sphingolipid, arginine, and homocysteine metabolism.

Based on earlier literature, we have optimized PAH models as described in Hessel MHM et al.³⁰ We explored the monocrotaline-induced PAH model. The signs of illness began within 3–7 days after the induction of PAH which was associated with anorexia, failure to gain weight, and tachypnea. Further, histopathology of the pulmonary artery revealed significant thickening in the tunica intima, media, and adventitia of the pulmonary arterial wall. These cellular changes have been described in earlier studies that confirmed the development of the PAH model.^{31–33} Hence, after confirming these PAH-related changes, we performed a metabolomics analysis.

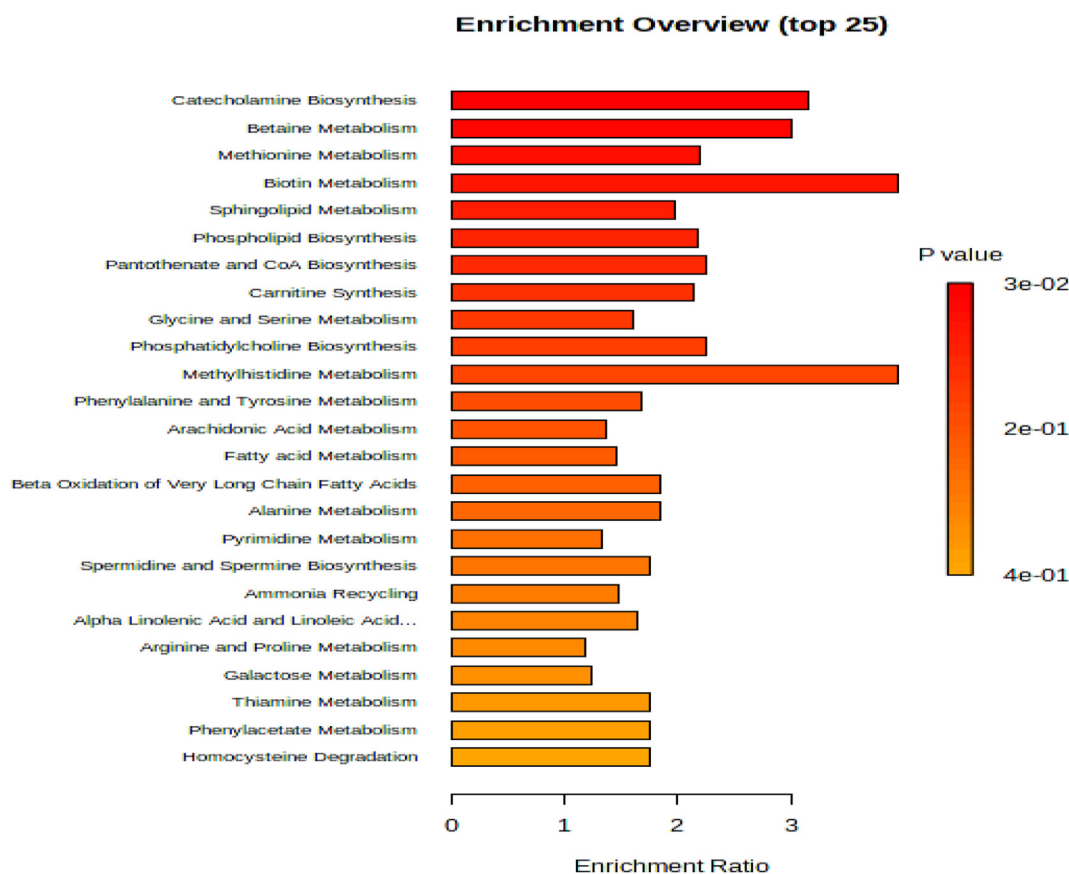


Fig. 6. Pathway enrichment analysis indicates PAH and exercise effects lipid and amino acid metabolism. The length of each column, which represents a particular metabolic path, reveals the enrichment ratio.

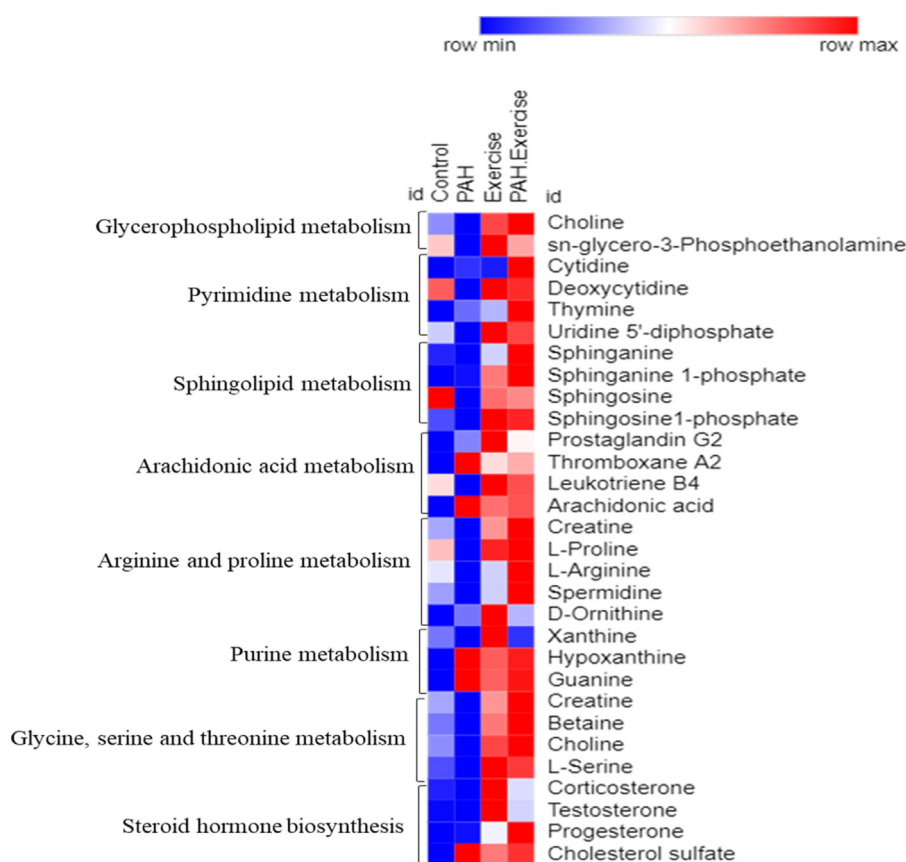


Fig. 7. Heat map representing the differential expression of significant endogenous metabolites across 4 different groups by average abundance in a single individual pathway.

NMR-based serum metabolomics analysis in monocrotaline-induced PAH in rats revealed methionine metabolism, glycolysis, ketogenesis, lipid metabolism, and energy metabolism suggesting a role of metabolic dysfunction in the PAH progression.³¹ Proteomics and metabolomics analysis in right ventricle tissue in PAH rats identified significant pathophysiological changes including elevated intracellular Ca^{2+} concentrations, inflammation, ferroptosis, mitochondrial metabolic shift, and insulin resistance.³² Authors demonstrated changes in glutathione and lipid peroxidation metabolism during the progression of PAH.³² In another PAH model, (i.e., the combination of monocrotaline and aortocaval shunting), metabolomic analysis of the pulmonary artery and right ventricle tissues revealed significant upregulation of pyrimidine and purine metabolism intermediates such as adenine, xanthosine, xanthine, hypoxanthine, deoxyadenosine, deoxyinosine, cytidine, thymine and others.³⁴ Taken together, the aforementioned metabolomic studies from different tissues revealed distinct modulations of metabolic pathways, suggesting PAH exerted tissue-specific metabolic reprogramming in vessel walls and systemic levels. Metabolomic analysis in our study also showed differences in lipid species, amino acids, and their derivatives and nucleotides. Patients with PAH had considerably higher serum levels of XOR (xanthine oxidoreductase), an enzyme that is known to catalyse the oxidation of hypoxanthine to xanthine and xanthine to Uric acid.³⁵ Nucleotide metabolism, a crucial mechanism that produces pyrimidine and purine molecules for DNA synthesis and replication, includes the metabolism of pyrimidines and purines. Plasma levels of purine metabolites, such as xanthine, xanthosine, uric acid, and others, have been found to be elevated in PAH, indicating enhanced oxidative stress. Additionally, it has been shown that the degree of PAH and Right ventricle (RV) dysfunction is correlated with plasma levels of purine metabolites. A recent study showed xanthine level was significantly altered in the PAH group compared to the control group.³⁶ These

observations were in agreement with our findings as we found Xanthine, Hypoxanthine, 1-Methylhypoxanthine, and guanine significantly altered in PAH.

Both preclinical and human data shows that exercise exerts beneficial effects on metabolism. Plasma profiling of human subjects who underwent resistance and endurance exercises showed mode-specific metabolic reprogramming.³⁷ Analysis at the resting phase before exercise, 1-h and 3-h post-exercise bout in both resistance and endurance modes showed increased circulating levels of metabolic intermediates related to cellular energy metabolism (glycolysis and TCA cycle) which included b-amino-isobutyric acid, 12, 13 DiHOME, succinate, lactate, and α -ketoglutarate and authors also showed elevated levels of kynurenine, a tryptophan metabolism intermediate.³⁷ This was also observed in our analysis in rats with exercise training. Another study showed time-dependent changes in systemic metabolism where authors identified metabolite indicators of glycogenolysis, TCA cycle, and lipolysis pathways. Further, the authors demonstrated circulating levels of glycerol was strongly correlated to fitness parameters.³⁸ The enzyme AMP-activated protein kinase (AMPK) is crucial for its role in nutrient sensing and energy homeostasis and dysfunction of AMPK decreases exercise capacity and impairs metabolism. Plasma metabolomics analysis in wild-type and AMPK-double knock-out mice with or without exercise revealed significant metabolic reprogramming influencing amino acid and pantothenic acid levels contributing to fuel utilization.³⁹ Interestingly, our data also showed modulations in signatures associated with levels of Pantetheine 4'-phosphate significantly decreased in the exercise group. In a rat model of depression, aerobic exercise led to improvement in depression-like behaviour and differential regulation of metabolites associated with amino acid and energy metabolism, shedding light on the metabolic mechanisms underlying the antidepressant effects of exercise.⁴⁰

Comparative analysis of metabolite signatures between PAH and PAH-exercise rats revealed that exercise significantly restored metabolism in PAH animals. Cer(d18:0/16:0) levels have been associated with the development and progression of atherosclerosis and cardiovascular disease's potential link to risk.^{41,42} Interestingly, ceramide levels were restored with exercise in PAH animals. Similarly, Leukotriene B4 levels were decreased in the PAH group and significantly altered with exercise. Previous research reported elevated LTB4 and myeloperoxidase (MPO) levels within three days of MCT injection in rats.⁴³ Therapeutic interventions in SU5416 combined with hypoxia (SuHx) rats similarly suppressed changes in phosphatidylcholine (PC) and lysophospholipids (LysoPC). However, the role of altered phospholipid metabolism in PAH etiology and RV remodelling is unclear.⁴⁴ PH is associated with significant alterations in plasma lysophosphatidic acid (LPA), which may influence the pathophysiology of PH.⁴⁵ Acute hypoxic pulmonary vasoconstriction (HPV) depends on diacylglycerol (DAG) via transient receptor potential 6 (TRPC6).⁴⁶ The accumulation of triglycerides (TAG), DAG, and ceramides is linked to insulin resistance, cardiac dysfunction, and right heart failure.^{47–50} Treatment targets for cardiovascular disease (CVD) may include circulating Monoacylglycerols (MAG), lysophosphatidic acids (LPA), and lysophospholipids (LPL).⁴⁵ In our study, LysoPC, LPA, DG, and LysoPE levels were significantly reduced in the PAH group compared to the control group and subsequently, increased in PAH upon exercising. In a recent study, it was seen that the right ventricle and pulmonary arteries share a dysregulated mechanism for glycerophospholipid metabolism in PAH. Furthermore, they had lower levels of phosphorylcholine, dihydroxyacetone phosphate, O-phospho ethanolamine, lecithin, and 1-palmitoyl-*sn*-glycero-3-phosphocholine, indicating that glycerophospholipid metabolism had been downregulated in PAH.³⁴ We observed 1-Palmitoylphosphatidylcholine, Choline, Cer(d18:0/12:0), LysoPE, and LysoPC were significantly downregulated in the PAH group. Downregulation of glycerophospholipid metabolism in PAH causes an increase in oxidative stress by controlling the inflammatory response and functioning as a crucial element in the pulmonary vascular remodelling process.^{34,51–53} Arachidonic metabolites, Thromboxane A2, Arachidonic acid, and Prostaglandin G2 were upregulated in the PAH group compared to the control group. Dysregulation of this pathway and the resulting imbalances in these metabolites have significant implications for the development and progression of PAH, impacting pulmonary blood vessel constriction, inflammation, vasodilation, clot formation, and vascular function.^{54–57} A recent study shows that analysis of the lung tissue from patients with PAH revealed significant alterations in the metabolism of sphingolipid and sphingolipid metabolites.⁵⁸ Hypoxia-induced PAH model also showed alterations in sphingolipid metabolism.⁵⁹ Interestingly, we observed exercise restored sphingolipid metabolic intermediates. Taken together, this suggests that exercise has beneficial effects on lipid metabolism in PAH models.

In addition, we identified changes to homocysteine and arginine, which are important metabolites that are involved maintaining vascular function.^{60,61} Homocysteine has been shown to inhibit dimethylarginine dimethylaminohydrolase (DDAH), an enzyme crucial for metabolizing asymmetric dimethylarginine (ADMA),⁶² which, in turn, inhibits nitric oxide (NO) synthase.^{63,64} Nitric oxide (NO) synthase facilitates the production of the vasodilator nitric oxide (NO) from L-arginine.⁶² Therefore, elevated homocysteine levels may reduce NO bioavailability.⁶⁵ This impact could be more pronounced in PAH patients, as they may already exhibit low NO levels, as suggested by prior studies.⁶⁶ In our study, homocysteine levels were significantly increased in the PAH group, which decreased with exercise. This suggests that exercise interventions might potentially help reduce homocysteine levels⁶⁷ and thereby improve vascular function. However, more comprehensive, and specific studies are needed to precisely determine the impact of exercise on homocysteine levels in individuals diagnosed with PAH.

L-arginine is a precursor to NO⁶¹ which is impaired in PAH.⁶⁸ When Arginase, an enzyme that turns arginine into ornithine and urea, competes with NOS for arginine, NO expression is reduced.⁶⁹ In PAH, the

decline in NO production is linked to two key mechanisms: (i) endothelial nitric oxide synthase (eNOS) inactivation through phosphorylation, and (ii) heightened mitochondrial Arginase2 causing reduced arginine availability, a vital eNOS substrate. These processes collectively contribute to impair NO synthesis in PAH.⁷⁰ In our study, reduced levels of L-arginine and L-phosphoarginine and a simultaneous increase of D-Ornithine were observed in PAH, which were restored with exercise. A recent study found the potential benefits of exercise on nitric oxide-mediated pulmonary artery vasorelaxation in male rats. Additionally, acute L-arginine supplementation in male rats was found to enhance acetylcholine-induced vasorelaxation.⁷¹ Another study indicated that a prescribed home-based walking routine alongside arginine supplementation in clinically stable PAH patients resulted in comparable improvements in function and quality of life (QoL) similar to more structured exercise programs.⁷²

Therefore, a comprehensive clinical study on a large scale is necessary to establish the benefits of homocysteine and arginine as a definitive biomarker for the diagnosis and prognosis of PAH. Future studies should consider an in-depth assessment of pathways and dose-response relationships on metabolism in PAH to better understand the most beneficial exercise training.

5. Conclusions

In conclusion, this study highlights the significance and metabolic basis of exercise training in improving PAH. The metabolomic analysis of PAH plasma contributes to a comprehensive understanding of the underlying mechanisms involved in PAH pathogenesis, particularly by identifying dysregulated metabolism, such as lipid metabolism, amino acid, and nucleotide metabolism. The disrupted arginine pathway altered sphingolipid metabolites, glycerophospholipid metabolism, and elevated homocysteine levels may provide insights into the severity and outcome of the disease. On the other hand, restored metabolic intermediates as a consequence of exercise may facilitate the design of therapeutic strategies by supplementing these key metabolites in PAH subjects who are unable to undergo exercise training. Taken together, our study provides novel insights into PAH and exercise biology.

Funding

GP was supported by the Senior Research Fellowship from the Indian Council of Medical Research, Govt of India through the research grant to ASB. This work was supported by an extramural research grant from the Indian Council of Medical Research to ASB (5/4/1–9/2019-NCD-II). SV was financially supported by Dr. TMA Pai Fellowship from Manipal Academy of Higher Education, Manipal.

Ethical approval statement

All animal experiments were performed in accordance with institutional animal ethics committee of Kasturba Medical College, Manipal Academy of Higher Education, Manipal (IAEC/KMC/41/2019). And “No human studies were carried out by the authors for this article”.

CRedit authorship contribution statement

Ganesh Poojary: Writing – review & editing, Writing – original draft, Methodology, Formal analysis, Data curation. **Sampara Vasishtha:** Writing – review & editing, Formal analysis, Data curation. **R. Huban Thomas:** Writing – review & editing, Methodology. **Kapaettu Satyamoorthy:** Writing – review & editing, Visualization, Supervision, Methodology, Investigation, Funding acquisition, Data curation, Conceptualization. **Ramachandran Padmakumar:** Writing – review & editing, Visualization, Supervision, Funding acquisition. **Manjunath B. Joshi:** Writing – review & editing, Writing – original draft, Visualization, Supervision, Resources, Methodology, Investigation, Funding

acquisition, Data curation, Conceptualization. **Abraham Samuel Babu:** Writing – review & editing, Writing – original draft, Visualization, Supervision, Resources, Methodology, Investigation, Funding acquisition, Data curation, Conceptualization.

Conflict of interest

The authors declare that they have no known competing financial interests or personal relationships that could have appeared to influence the work reported in this paper.

Acknowledgments

The authors acknowledge the support from the Manipal Academy of Higher Education and the Manipal School of Lifesciences for the infrastructure.

Appendix A. Supplementary data

Supplementary data to this article can be found online at <https://doi.org/10.1016/j.smhs.2024.03.001>.

References

- Morrell NW, Adnot S, Archer SL, et al. Cellular and molecular basis of pulmonary arterial hypertension. *J Am Coll Cardiol*. 2009;54(1 suppl):S20–S31. <https://doi.org/10.1016/j.jacc.2009.04.018>.
- Simonneau G, Robbins IM, Beghetti M, et al. Updated clinical classification of pulmonary hypertension. *J Am Coll Cardiol*. 2009;54(1 suppl):S43–S54. <https://doi.org/10.1016/j.jacc.2009.04.012>.
- Farber HW, Miller DP, McGoon MD, Frost AE, Benton WW, Benza RL. Predicting outcomes in pulmonary arterial hypertension based on the 6-minute walk distance. *J Heart Lung Transplant*. 2015;34(3):362–368. <https://doi.org/10.1016/j.healun.2014.08.020>.
- Paulin R, Michelakis ED. The metabolic theory of pulmonary arterial hypertension. *Circ Res*. 2014;115(1):148–164. <https://doi.org/10.1161/CIRCRESAHA.115.301130>.
- Ball MK, Waypa GB, Mungai PT, et al. Regulation of hypoxia-induced pulmonary hypertension by vascular smooth muscle hypoxia-inducible factor-1 α . *Am J Respir Crit Care Med*. 2014;189(3):314–324. <https://doi.org/10.1164/rccm.201302-0302OC>.
- Yu AY, Shimoda LA, Iyer NV, et al. Impaired physiological responses to chronic hypoxia in mice partially deficient for hypoxia-inducible factor 1 α . *J Clin Invest*. 1999;103(5):691–696. <https://doi.org/10.1172/JCI5912>.
- Heiden MG, Cantley LC, Thompson CB. Understanding the warburg effect: the metabolic requirements of cell proliferation. *Science*. 2009;324(5930):1029–1033. <https://doi.org/10.1126/science.1160809>.
- Bonnet S, Michelakis ED, Porter CJ, et al. An Abnormal mitochondrial-hypoxia inducible factor-1 α -Kv channel pathway disrupts oxygen sensing and triggers pulmonary arterial hypertension in fawn hooded rats: Similarities to human pulmonary arterial hypertension. *Circulation*. 2006;113(22):2630–2641. <https://doi.org/10.1161/CIRCULATIONAHA.105.609008>.
- Mainguy V, Maltais F, Saey D, et al. Peripheral muscle dysfunction in idiopathic pulmonary arterial hypertension. *Thorax*. 2010;65(2):113–117. <https://doi.org/10.1136/thx.2009.117168>.
- Tuder RM, Chacon M, Alger L, et al. Expression of angiogenesis-related molecules in plexiform lesions in severe pulmonary hypertension: evidence for a process of disordered angiogenesis. *J Pathol*. 2001;195(3):367–374. <https://doi.org/10.1002/path.953>.
- Fijalkowska I, Xu W, Comhair SAA, et al. Hypoxia inducible-factor1 α regulates the metabolic shift of pulmonary hypertensive endothelial cells. *Am J Pathol*. 2010;176(3):1130–1138. <https://doi.org/10.2353/ajpath.2010.090832>.
- Li M, Riddle S, Zhang H, et al. Metabolic reprogramming regulates the proliferative and inflammatory phenotype of adventitial fibroblasts in pulmonary hypertension through the transcriptional corepressor C-terminal binding protein-1. *Circulation*. 2016;134(15):1105–1121. <https://doi.org/10.1161/CIRCULATIONAHA.116.023171>.
- Drake JI, Bogaard HJ, Mizuno S, et al. Molecular signature of a right heart failure program in chronic severe pulmonary hypertension. *Am J Respir Cell Mol Biol*. 2011;45(6):1239–1247. <https://doi.org/10.1165/rccm.2010-0412OC>.
- Malenfant S, Potus F, Fournier F, et al. Skeletal muscle proteomic signature and metabolic impairment in pulmonary hypertension. *J Mol Med*. 2015;93(5):573–584. <https://doi.org/10.1007/s00109-014-1244-0>.
- Fessel JP, Hamid R, Wittmann BM, et al. Metabolomic analysis of bone morphogenetic protein receptor type 2 mutations in human pulmonary endothelium reveals widespread metabolic reprogramming. *Pulm Circ*. 2012;2(2):201–213. <https://doi.org/10.4103/2045-8932.97606>.
- Zhang H, Wang D, Li M, et al. Metabolic and proliferative state of vascular adventitial fibroblasts in pulmonary hypertension is regulated through a MicroRNA-124/PTBP1 (Polypyrimidine tract binding protein 1)/Pyruvate kinase muscle axis. *Circulation*. 2017;136(25):2468–2485. <https://doi.org/10.1161/CIRCULATIONAHA.117.028069>.
- Archer SL, Gomberg-Maitland M, Maitland ML, Rich S, Garcia JGN, Kenneth Weir E. Mitochondrial metabolism, redox signaling, and fusion: a mitochondria-ROS-HIF-1-Kv1.5 O₂-sensing pathway at the intersection of pulmonary hypertension and cancer. *Am J Physiol Heart Circ Physiol*. 2008;294(2):570–578. <https://doi.org/10.1152/ajpheart.01324.2007>.
- Pi H, Xia L, Ralph DD, et al. Metabolomic signatures associated with pulmonary arterial hypertension outcomes. *Circ Res*. 2023;132(3):254–266. <https://doi.org/10.1161/CIRCRESAHA.122.321923>.
- Chen C, Luo F, Wu P, et al. Metabolomics reveals metabolite changes of patients with pulmonary arterial hypertension in China. *J Cell Mol Med*. 2020;24(4):2484–2496. <https://doi.org/10.1111/jcmm.14937>.
- He YY, Yan Y, Jiang X, et al. Spermine promotes pulmonary vascular remodelling and its synthase is a therapeutic target for pulmonary arterial hypertension. *Eur Respir J*. 2020;56(5):2000522. <https://doi.org/10.1183/13993003.00522-2020>.
- Babu AS, Arena R, Myers J, et al. Exercise intolerance in pulmonary hypertension: mechanism, evaluation and clinical implications. *Expert Rev Respir Med*. 2016;10(9):979–990. <https://doi.org/10.1080/17476348.2016.1191353>.
- Satyamurthy A, Poojary G, Dibben G, et al. Exercise Training in Pulmonary Hypertension - an updated systematic review with meta-analysis. *J Cardiopulm Rehabil Prev*. 2023;43(4):237–244. <https://doi.org/10.1097/HCR.0000000000000765>.
- Morris NR, Kermeen FD, Holland AE. Exercise-based rehabilitation programmes for pulmonary hypertension. *Cochrane Database Syst Rev*. 2017;2017(1):CD011285. <https://doi.org/10.1002/14651858.CD011285.pub2>.
- du Sert NP, Ahluwalia A, Alam S, et al. Reporting animal research: Explanation and elaboration for the arrive guidelines 2.0. *PLoS Biol*. 2020;18(7):e3000411. <https://doi.org/10.1371/journal.pbio.3000411>.
- Handoko ML, de Man FS, Happé CM, et al. Opposite effects of training in rats with stable and progressive pulmonary hypertension. *Circulation*. 2009;120(1):42–49. <https://doi.org/10.1161/CIRCULATIONAHA.108.829713>.
- Joshi MB, Pai S, Balakrishnan A, et al. Evidence for perturbed metabolic patterns in bipolar disorder subjects associated with lithium responsiveness. *Psychiatry Res*. 2019;273:252–259. <https://doi.org/10.1016/j.psychres.2019.01.031>.
- Tautenhahn R, Patti GJ, Rinehart D, Siuzdak G. XCMS online: a web-based platform to process untargeted metabolomic data. *Anal Chem*. 2012;84(11):5035–5039. <https://doi.org/10.1021/ac300698c>.
- Chambers MC, MacLean B, Burke R, et al. A cross-platform toolkit for mass spectrometry and proteomics. *Nat Biotechnol*. 2012;30(10):918–920. <https://doi.org/10.1038/nbt.2377>.
- Ivanisevic J, Zhu ZJ, Plate L, et al. Toward 'Omic scale metabolite profiling: a dual separation-mass spectrometry approach for coverage of lipid and central carbon metabolism. *Anal Chem*. 2013;85(14):6876–6884. <https://doi.org/10.1021/ac401140h>.
- Hessel MHM, Steendijk P, Den Adel B, Schutte CI, Van Der Laarse A. Characterization of right ventricular function after monocrotaline-induced pulmonary hypertension in the intact rat. *Am J Physiol Heart Circ Physiol*. 2006;291(5):2424–2430. <https://doi.org/10.1152/ajpheart.00369.2006>.
- Lin T, Gu J, Huang C, et al. (1) H NMR-based analysis of serum metabolites in monocrotaline-induced pulmonary arterial hypertensive rats. *Dis Markers*. 2016;2016:5803031. <https://doi.org/10.1155/2016/5803031>.
- Qin X, Lei C, Yan L, et al. Proteomic and metabolomic analyses of right ventricular failure due to pulmonary arterial hypertension. *Front Mol Biosci*. 2022;9:834179. <https://doi.org/10.3389/fmolb.2022.834179>.
- Nogueira-Ferreira R, Vitorino R, Ferreira R, Henriques-Coelho T. Exploring the monocrotaline animal model for the study of pulmonary arterial hypertension: a network approach. *Pulm Pharmacol Ther*. 2015;35:8–16. <https://doi.org/10.1016/j.pupt.2015.09.007>.
- Liu D, Qin S, Su D, et al. Metabolic reprogramming of the right ventricle and pulmonary arteries in a flow-associated pulmonary arterial hypertension rat model. *ACS Omega*. 2022;7(1):1273–1287. <https://doi.org/10.1021/acsomega.1c05895>.
- Watanabe T, Abe K, Horimoto K, Hosokawa K, Ohtani K, Tsutsui H. Subcutaneous treprostinil was effective and tolerable in a patient with severe pulmonary hypertension associated with chronic kidney disease on hemodialysis. *Heart Lung*. 2017;46(2):129–130. <https://doi.org/10.1016/j.hrtlng.2017.01.004>.
- Lewis GD, Ngo D, Hemnes AR, et al. Metabolic profiling of right ventricular-pulmonary vascular function reveals circulating biomarkers of pulmonary hypertension. *J Am Coll Cardiol*. 2016;67(2):174–189. <https://doi.org/10.1016/j.jacc.2015.10.072>.
- Morville T, Sahl RE, Moritz T, Helge JW, Clemmensen C. Plasma metabolome profiling of resistance exercise and endurance exercise in humans. *Cell Rep*. 2020;33(13):108554. <https://doi.org/10.1016/j.celrep.2020.108554>.
- Lewis GD, Farrell L, Wood MJ, et al. Metabolic signatures of exercise in human plasma. *Sci Transl Med*. 2010;2(33):33ra37. <https://doi.org/10.1126/scitranslmed.3001006>.
- Belhaj MR, Lawler NG, Hawley JA, Broadhurst DI, Hoffman NJ, Reinke SN. Metabolomics reveals mouse plasma metabolite responses to acute exercise and effects of disrupting AMPK-glycogen interactions. *Front Mol Biosci*. 2022;9:957549. <https://doi.org/10.3389/fmolb.2022.957549>.
- Liu X, Han Y, Zhou S, et al. Serum metabolomic responses to aerobic exercise in rats under chronic unpredictable mild stress. *Sci Rep*. 2022;12(1):4888. <https://doi.org/10.1038/s41598-022-09102-2>.

41. Liu H, Chen X, Hu X, et al. Alterations in the gut microbiome and metabolism with coronary artery disease severity. *Microbiome*. 2019;7(1):68. <https://doi.org/10.1186/s40168-019-0683-9>.
42. Havulinna AS, Sysi-Aho M, Hilvo M, et al. Circulating ceramides predict cardiovascular outcomes in the population-based FINRISK 2002 Cohort. *Arterioscler Thromb Vasc Biol*. 2016;36(12):2424–2430. <https://doi.org/10.1161/ATVBAHA.116.307497>.
43. Tian W, Jiang X, Sung YK, Qian J, Yuan K, Nicolls MR. Leukotrienes in pulmonary arterial hypertension. *Immunol Res*. 2014;58(2-3):387–393. <https://doi.org/10.1007/s12026-014-8492-5>.
44. Mamazhakypov A, Weiß A, Zukunft S, et al. Effects of macitentan and tadalafil monotherapy or their combination on the right ventricle and plasma metabolites in pulmonary hypertensive rats. *Pulm Circ*. 2020;10(4):2045894020947283. <https://doi.org/10.1177/2045894020947283>.
45. Duflet T, Tu L, Leuillier M, et al. Preventing the increase in lysophosphatidic acids: a new therapeutic target in pulmonary hypertension? *Metabolites*. 2021;11(11):1–18. <https://doi.org/10.3390/metabol11110784>.
46. Fuchs B, Rupp M, Ghofrani HA, et al. Diacylglycerol regulates acute hypoxic pulmonary vasoconstriction via TRPC6. *Respir Res*. 2011;12:1–10. <https://doi.org/10.1186/1465-9921-12-20>.
47. Hemnes AR, Brittain EL, Trammell AW, et al. Evidence for right ventricular lipotoxicity in heritable pulmonary arterial hypertension. *Am J Respir Crit Care Med*. 2014;189(3):325–334. <https://doi.org/10.1164/rccm.201306-1086OC>.
48. Noureddine L, Azzam R, Nemer G, et al. Modulation of total ceramide and constituent ceramide species in the acutely and chronically hypoxic mouse heart at different ages. *Prostaglandins Other Lipid Mediat*. 2008;86(1-4):49–55. <https://doi.org/10.1016/j.prostaglandins.2008.02.003>.
49. Ouwens DM, Boer C, Fodor M, et al. Cardiac dysfunction induced by high-fat diet is associated with altered myocardial insulin signalling in rats. *Diabetologia*. 2005;48(6):1229–1237. <https://doi.org/10.1007/s00125-005-1755-x>.
50. Heresi GA, Aytakin M, Newman J, DiDonato J, Dweik RA. Plasma levels of high-density lipoprotein cholesterol and outcomes in pulmonary arterial hypertension. *Am J Respir Crit Care Med*. 2010;182(5):661–668. <https://doi.org/10.1164/rccm.20101001-0007OC>.
51. Dang VT, Zhong LH, Huang A, Deng A, Werstuck GH. Glycosphingolipids promote pro-atherogenic pathways in the pathogenesis of hyperglycemia-induced accelerated atherosclerosis. *Metabolomics*. 2018;14(7):92. <https://doi.org/10.1007/S11306-018-1392-2>.
52. Cui Y, Liu S, Zhang X, et al. Metabolomic analysis of the effects of adipose-derived mesenchymal stem cell treatment on rats with sepsis-induced acute lung injury. *Front Pharmacol*. 2020;11:902. <https://doi.org/10.3389/fphar.2020.00902>.
53. Zhu T, Li S, Wang J, et al. Induced sputum metabolomic profiles and oxidative stress are associated with chronic obstructive pulmonary disease (COPD) severity: potential use for predictive, preventive, and personalized medicine. *EPMA J*. 2020;11:645–659. <https://doi.org/10.1007/s13167-020-00227-w>.
54. Park SJ, Yoo HY, Earm YE, Kim SJ, Kim JK, Kim SD. Role of arachidonic acid-derived metabolites in the control of pulmonary arterial pressure and hypoxic pulmonary vasoconstriction in rats. *Br J Anaesth*. 2011;106(1):31–37. <https://doi.org/10.1093/bja/aeq268>.
55. Alqarni AA. Increased thromboxane a2 levels in pulmonary artery smooth muscle cells isolated from patients with chronic obstructive pulmonary disease. *Medicina (Lithuania)*. 2023;59(1):165. <https://doi.org/10.3390/medicina59010165>.
56. Zhou Y, Khan H, Xiao J, Cheang WS. Effects of arachidonic acid metabolites on cardiovascular health and disease. *Int J Mol Sci*. 2021;22(21):12029. <https://doi.org/10.3390/ijms222112029>.
57. Ricciotti E, Fitzgerald GA. Prostaglandins and inflammation. *Arterioscler Thromb Vasc Biol*. 2011;31(5):986–1000. <https://doi.org/10.1161/ATVBAHA.110.207449>.
58. Zhao YD, Chu L, Lin K, et al. A biochemical approach to understand the pathogenesis of advanced pulmonary arterial hypertension: metabolomic profiles of arginine, sphingosine-1-phosphate, and heme of human lung. *PLoS One*. 2015;10(8):1–13. <https://doi.org/10.1371/journal.pone.0134958>.
59. Chen J, Tang H, Sysol JR, et al. The sphingosine kinase 1/sphingosine-1-phosphate pathway in pulmonary arterial hypertension. *Am J Respir Crit Care Med*. 2014;190(9):1032–1043. <https://doi.org/10.1164/rccm.201401-0121OC>.
60. Karger AB, Steffen BT, Nomura SO, et al. Association between homocysteine and vascular calcification incidence, prevalence, and progression in the MESA cohort. *J Am Heart Assoc*. 2020;9(3):e013934. <https://doi.org/10.1161/JAHA.119.013934>.
61. Gambardella J, Khondkar W, Morelli MB, Wang X, Santulli G, Trimarco V. Arginine and endothelial function. *Biomedicines*. 2020;8(8):277. <https://doi.org/10.3390/BIMEDICINES8080277>.
62. Warwick J, Thomas PS, Yates DH. Biomarkers in pulmonary hypertension. *Eur Respir J*. 2008;32(2):503–512. <https://doi.org/10.1183/09031936.00160307>.
63. Böger RH. Asymmetric dimethylarginine (ADMA): a novel risk marker in cardiovascular medicine and beyond. *Ann Med*. 2006;38(2):126–136. <https://doi.org/10.1080/0785389050047215>.
64. Chatterjee A, Catravas JD. Endothelial nitric oxide (NO) and its pathophysiologic regulation. *Vascul Pharmacol*. 2008;49(4-6):134–140. <https://doi.org/10.1016/j.vph.2008.06.008>.
65. Giaid A. Nitric oxide and endothelin-1 in pulmonary hypertension. *Chest*. 1998;114(3 Suppl):208S–212S. https://doi.org/10.1378/chest.114.3_Supplement.208S.
66. Millatt LJ, Whitley GSJ, Li D, et al. Evidence for dysregulation of dimethylarginine dimethylaminohydrolase I in chronic hypoxia-induced pulmonary hypertension. *Circulation*. 2003;108(12):1493–1498. <https://doi.org/10.1161/01.CIR.0000089087.25930.FF>.
67. Okura T, Rankinen T, Gagnon J, et al. Effect of regular exercise on homocysteine concentrations: the HERITAGE Family Study. *Eur J Appl Physiol*. 2006;98(4):394–401. <https://doi.org/10.1007/s00421-006-0294-6>.
68. Klinger JR, Abman SH, Gladwin MT. Nitric oxide deficiency and endothelial dysfunction in pulmonary arterial hypertension. *Am J Respir Crit Care Med*. 2013;188(6):639–646. <https://doi.org/10.1164/rccm.201304-0686PP>.
69. Maarsingh H, Pera T, Meurs H. Arginase and pulmonary diseases. *Naunyn-Schmiedeberg's Arch Pharmacol*. 2008;378(2):171–184. <https://doi.org/10.1007/s00210-008-0286-7>.
70. Xu W, Janocha AJ, Erzurum SC. Metabolism in pulmonary hypertension. *Annu Rev Physiol*. 2021;83:551–576. <https://doi.org/10.1146/annurev-physiol-031620-123956>.
71. Goret L, Tanguy S, Guiraud I, Dauzat M, Obert P. Acute administration of L-arginine restores nitric oxide-mediated relaxation in isolated pulmonary arteries from pulmonary hypertensive exercise trained rats. *Eur J Pharmacol*. 2008;581(1-2):148–156. <https://doi.org/10.1016/j.ejphar.2007.11.037>.
72. Brown MB, Kempf A, Collins CM, et al. A prescribed walking regimen plus arginine supplementation improves function and quality of life for patients with pulmonary arterial hypertension: a pilot study. *Pulm Circ*. 2018;8(1):2045893217743966. <https://doi.org/10.1177/2045893217743966>.